Time Delay and Gain Reduction in Reflective Semiconductor Optical Amplifier

Jacques W. D. Chi

Time Delay and Gain Reduction in Reflective Semiconductor Optical Amplifier

(Invited paper)

Jacques W. D. Chi

***Abstract*—Amplification of picosecond optical pulses by reflective semiconductor optical amplifier (RSOA) is theoretically investigated using a high-precision time-domain model. It is demonstrated that, compared to conventional SOA in similar conditions, pulses amplified by RSOA suffer from additional gain reduction of a few dB due to RSOA's rear-facet reflection, which increases saturation level inside the device. The time delay and waveform of output pulse could be very different from RSOA or SOA providing the same small-signal gain. The model is then applied to a 40 Gb/s PCM signal to study the patterning effect in both SOA and RSOA.**

***Index Terms*—Optical pulses, reflective semiconductor optical amplifier (RSOA), time-domain modeling, patterning effect.**

I. Introduction

As a compact, effective and versatile amplification device, semiconductor optical amplifier (SOA) has shown its potential in many applications, including optical pulse generation and amplification, as well as communication networks. Compared to a conventional SOA, reflective SOAs (RSOAs) provide some interesting features [1]-[3]. In effect, a RSOA doubles the length of the gain medium of a SOA, offering therefore a higher small-signal optical gain with the same drive current. The drawback is that a RSOA is more easily saturated, because the injected and reflected optical waves share the same pool of inversed carriers. The nonlinear interaction between these two waves in a dynamic gain medium makes it difficult to analytically obtain the amplified output signal, in contrast to a SOA where analytical predictions are possible in some situations [4]. As a consequence, numerical simulations are necessary for RSOA. Indeed, in a recent study [3], interaction between relatively slow (~50 ps) injected and reflected optical pulses in RSOA is investigated using a first-order numerical approach.

In order to predict reliably the behaviors of RSOA, especially for shorter pulses (a few ps in width) with relatively high intensities compared to the saturation power of RSOA, we adept a newly developed high-order (4^{th}) numerical model [5] to RSOA. The model has shown excellent agreement with both analytical and experimental results in SOA [6]. Since the only difference between the RSOA, studied in this paper, and the configuration in [6] is the replacement of the optical back injection in the SOA by the rear-mirror reflection in the RSOA, the high precision demonstrated in [6] should be retained here.

It is well known that both SOA and RSOA are prone to inter-symbol interference, or the patterning effect [7], which originates from incomplete gain recovery when amplifying a fast pulse train. In the case of RSOA, moreover, a reflected pulse may overlap with the next upcoming pulse in the active medium. Although this effect might be avoidable in applications with moderate bit-rates (≤10 Gb/s) and fast components such as in [6], it remains highly desirable to develop an accurate simulation tool capable of handling this effect, which is one of the main concerns for the deployment of SOA or RSOA in practical applications involving fast signals. In this paper, we show that the present model is readily applicable to this patterning effect, by demonstrating the amplification of a 40 Gb/s coded pulse train by both SOA and RSOA.

In the following, we will firstly focus on pulse amplification behavior due to intrinsic effects in SOA/RSOA. Secondly, the model will be applied to a 8-bits coded pulse stream. The aim is to provide a high-precision modeling tool when bulk- and MQW-RSOAs are adopted in applications mentioned above.

II. RSOA Model and Numerical Procedure

In this paper, we consider the situation of input optical signals far stronger than the noise level in both SOA and RSOA. In addition, the frequency bandwidths are narrow enough (~ 1nm) for both input and amplified output signals, as is the case for picosecond optical pulses. It is therefore justified to ignore the noise and other wideband effects [8]. In such conditions, the contra-propagating slowly-varying field envelops could be described by the phenomenological model under $-i\omega t$ convention as [4]:

$$\pm\partial_z A^{\pm} + v_g^{-1}\partial_t A^{\pm} = \frac{1}{2} g(1 - i\alpha_H) A^{\pm}, \qquad (1)$$

The author is with the Ecole Nationale d'Ingénieurs de Brest (ENIB), Laboratory DIM/Lab-STICC, CP. 29608, Brest, France (phone : +33 298 056636; fax: +33 298 056689; email: chi@enib.fr).

$$\partial_t g = \frac{g_0 - g}{\tau_c} - g\frac{\left(\left|A^+\right|^2 + \left|A^-\right|^2\right)}{E_{sat}}. \qquad (2)$$

Here, $A^{\pm}$ are the injected (+z) and reflected (-z) field envelops, respectively; v_g is the group velocity, g is the net optical (intensity) gain, g_0 is the small-signal gain, α_H is the Henry factor, τ_c is the carrier lifetime, E_{sat} is the saturation energy. The device length L=1 mm, corresponding to a small-signal transit delay of 13.3 ps for SOA, and 26.6 ps for RSOA, respectively. All parameters other than variables ($A^{\pm}$ and g) are assumed to be constant. The boundary conditions are R_1 (field reflectivity)=0 and R_2=1 at RSOA's two facets. The comparison with SOA is carried out using the same set of parameters except R_2=0.

The coupled equations (1)-(2) can be resolved numerically with high precision. In effect, we have developed a method which, firstly, transforms the system (1)-(2) into pseudo-ordinary differential equations by introducing new coordinates ($v_g t \pm z$)/2 to substitute (t, z), and then applies a predictor-corrector scheme in the new coordinate frame. The outcome is equivalent to the well-known 4th-order Runge-Kutta algorithm in terms of stability and convergence. The technical details and verifications are available in [5]. The procedure is applied to a mode-locked laser using SOA as described above in [6], where excellent agreement is obtained between theoretical prediction and experiment. The adaptation of the algorithm in [5] to RSOA is straightforward, by noticing that the boundary condition at z=L is now A^-=R_2A^+. This numerical procedure could easily be extended to include the effects of residual facet reflection, gain dispersion [5], spectral hole-burning [3], as well as the patterning and overlapping mentioned above. Notice, however, that the model (1)-(2) itself may be questionable if the signal becomes too fast (~1 ps or less).

III. AMPLIFICATION OF A SINGLE PULSE

In order to compare the behaviors of RSOA and SOA, one has to match their parameters as closely as possible. We choose a commercially-available SOA (CIP, SOA-NL-OEC) as reference, since its parameters are checked at λ=1.55 μm in [6]. The corresponding RSOA is not available yet (to our knowledge), but should be technologically possible. In the following we use E_{sat}=0.5 pJ, τ_c=16 ps, v_g=c/4, α_H =6, and the small-signal gain is fixed at 28dB for both SOA and RSOA. This gain is obtained at 290 mA bias in SOA [6], accompanied by a noise (ASE) level of -26 dBm/nm. Since a uniform carrier density is assumed at steady-state, the difference in length or in drive current between SOA and RSOA are transparent in this model, as long as they provide the same small-signal gain. Note also that, since many device parameters are dependent on carrier density, it may be easier to match SOA and RSOA with L_{SOA}=2×L_{RSOA}.

Let's consider the amplification of two Gaussian pulses of different widths by SOA and RSOA, respectively. The first τ_1=5 ps (FWHM) is fast compared to the carrier lifetime, the second τ_2=30 ps is relatively slow. The optical intensity of these pulses is calibrated with the saturation power P_{sat} of SOA/RSOA, defined as P_{sat}=E_{sat}/τ_c (≈31 mW here). The peak input intensity is P_0. We consider weak (P_0/P_{sat}=0.1), moderate (P_0/P_{sat}=1) and strong (P_0/P_{sat}=10) input intensities.

The amplification of weak pulses (P_0/P_{sat}=0.1) are shown in Fig. 1. The waveforms in (1a) and (1c) are traced in a time coordinate moving at the group velocity, such that the origin (t=0) will indicate the pulses' peak position if the small-signal (linear) amplification is observed. It can be seen that, although the input intensity is relatively weak, the typical effect of nonlinear distortion is already present. For the short (τ_1=5 ps) pulse, the time delay is nearly the same for both SOA and RSOA, but a reduced peak power (~13 percent lower or -0.6 dB) from RSOA is observed, due to its stronger saturation. For the long (τ_2=30 ps) pulse shown in Fig. (1c), this gain penalty on RSOA is more severe (-1.6 dB), where the leading edge of the RSOA-amplified pulse saturates more quickly, resulting in a seemingly shorter time delay. The effect of carrier re-pumping is also visible at the trailing edge of the same pulse, but not with SOA. In spite of these differences in waveforms, the spectra from SOA and RSOA are very similar in structure and in bandwidth, for both the short and the long pulses. It can be easily checked that the ASE noise is not a concern at this input level, as long as the detection bandwidth is appropriate.

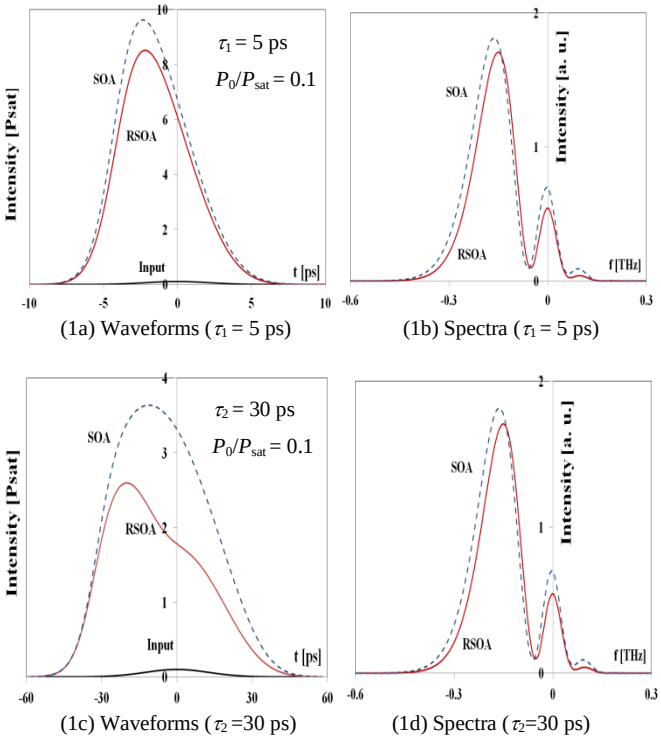

(1a) Waveforms (τ_1 = 5 ps) (1b) Spectra (τ_1 = 5 ps)

(1c) Waveforms (τ_2 =30 ps) (1d) Spectra (τ_2=30 ps)

Fig. 1. Waveforms and corresponding spectra of amplified pulses by SOA and RSOA with P_0/P_{sat}=0.1. (1a) and (1b): input Gaussian width τ_1=5 ps (FWHM); (1c) and (1d): τ_2=30 ps. Time coordinate is moving at v_g along with pulses' leading edges in (1a) and (1c). Idem for Figs. 2 and 3.

Fig. 2 illustrates the situation of moderate input intensity (P_0/P_{sat}=1). Compared to SOA, the gain reduction in RSOA is -1.1 dB for the short pulse, and -1.8 dB for the long one. In both cases, the RSOA amplification results in longer time delay, albeit for different reasons. For the short pulse, the leading edge

in the SOA gets higher amplification and steepens much strongly, while the carrier re-pumping results in a bulged trailing edge for the long pulse in RSOA. The spectral similitude remains true, as in Fig. 1. Notice also that, as expected, the amplification factor (output peak intensity/input peak intensity) is greatly reduced compared to Fig. 1.

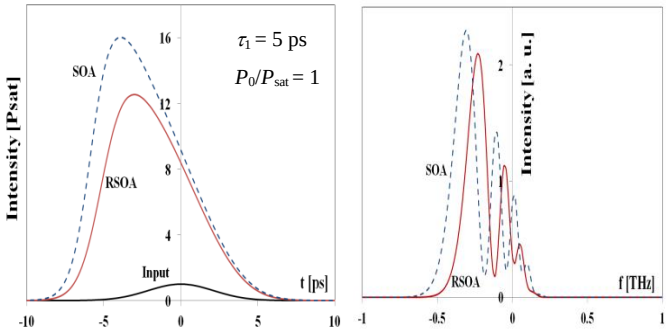

(2a) Waveforms (τ_1 = 5 ps) (2b) Spectra (τ_1 = 5 ps)

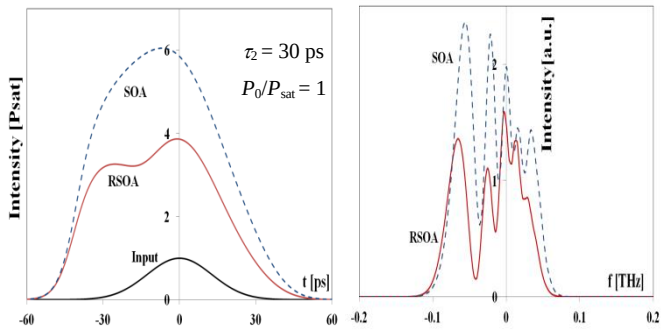

(2c) Waveforms (τ_2 =30 ps) (2d) Spectra (τ_2=30 ps)

Fig. 2. Amplified waveforms and corresponding spectra with P_0/P_{sat}=1. (2a) and (2b): τ_1=5 ps (FWHM); (2c) and (2d): τ_2=30 ps.

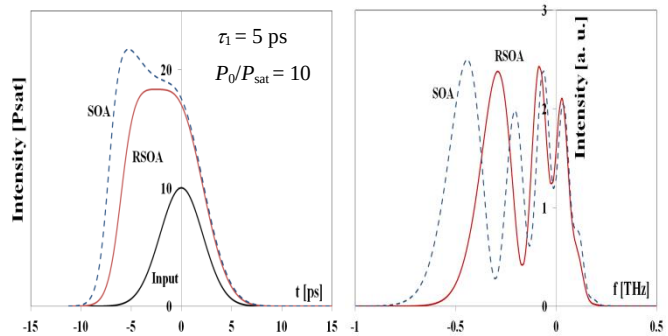

(3a) Waveforms (τ_1 = 5 ps) (3b) Spectra (τ_1 = 5 ps)

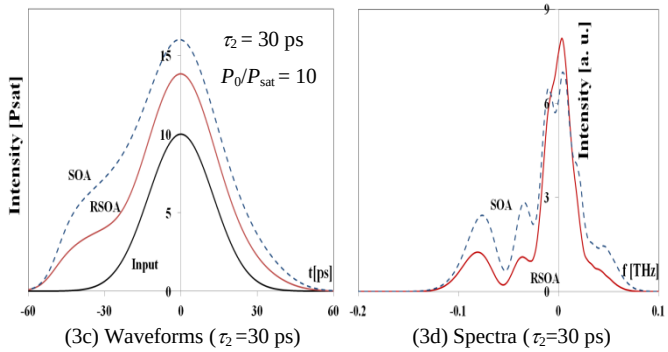

(3c) Waveforms (τ_2 =30 ps) (3d) Spectra (τ_2=30 ps)

Fig. 3. Amplified waveforms and corresponding spectra with P_0/P_{sat}=10. (3a) and (3b): τ_1=5 ps (FWHM); (3c) and (3d): τ_2=30 ps.

The situation of strong input intensity (P_0/P_{sat}=10) is shown in Fig. 3. Understandably, the amplification factor becomes still lower, since the output peak intensities are barely doubled for the short pulse in Fig. (3a), and even less for the long pulse in Fig. (3c). In this last case, the inversed carriers in both SOA and RSOA are quickly depleted by pulse's leading edge, leaving the re-pumped carriers to maintain the pulse waveform to the end. No additional time shift is observed in both SOA and RSOA amplifications. Notice that the relative gain reduction is always present in RSOA compared to SOA.

IV. Amplification of a Pulse Train

The above model and algorithm can be indifferently applied to any input signal, as long as its bandwidth is narrow enough (no more than a few nm) to avoid the effect of gain dispersion. As an example, we consider the amplification of a pulse train by both the SOA and the RSOA studied above. The input signal is a 40 Gb/s pulse stream 11100101, with "1" stands for a 10 ps (FWHM) Gaussian pulse, while "0" is fixed at constant -19 dB below the input intensity peaks to represent the noise level. To be consistent with the previous section, the maximum normalized intensity of the input pulses is set to be P_0/P_{sat}=0.1, 1, and 10, respectively. The device parameters are the same as in Section III. Notice that the incoming symbol period (25 ps) is comparable to the carrier lifetime (16 ps), as well as to the transit delays of the SOA (13.3 ps) or the RSOA (26.6 ps). The patterning effect is therefore unavoidable. The results are shown in Fig. 4.

Figs. 4(a)-4(c) show the amplification of the 8-bits signal with different input intensities. As expected, the patterning effect is obvious in all cases, and the SOA always provides more signal gain than the RSOA does. The waveform distortions are also observed and can be well explained by the single-pulse cases in Figs 1-3. Notice also that the noise performance would be different for SOA and RSOA, as can be observed from the gain recovery during "00" bits in the middle of the data stream. Interestingly, the patterning effect in Fig. 4(c) is reduced for both SOA and RSOA, albeit with moderate signal gains (~2dB).

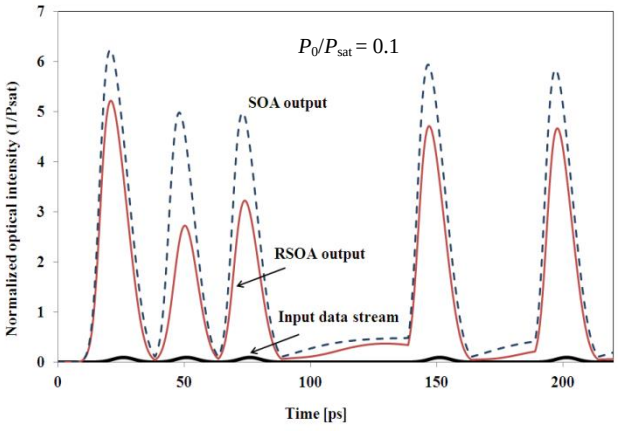

Fig. 4(a). Amplified pulse stream 11100101 by SOA and RSOA, respectively. The intensity maximum for input "1" is P_0/Psat=0.1, its minimum "0" is fixed at -19 dB below the input pulse peak to represent the noise level.

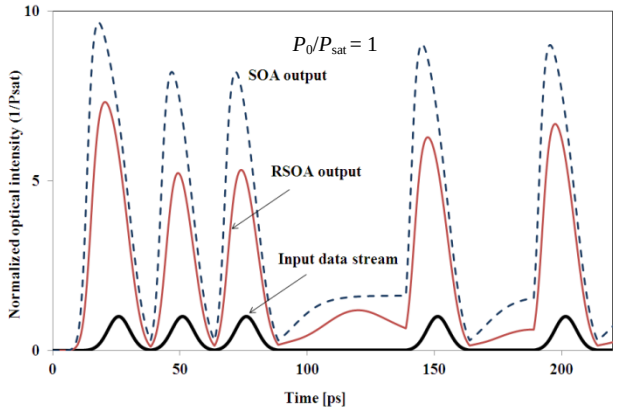

4(b). P_0/Psat=1.

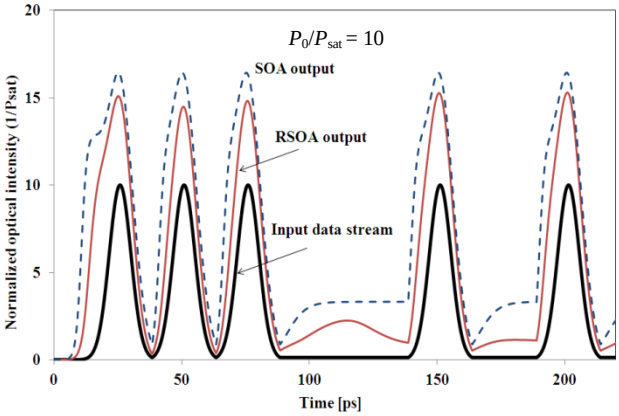

4(c). P_0/Psat=10.

V. Conclusion

Although Gaussian pulses are chosen as input signals for convenience, several broad observations could still be underlined. First and the most obvious is the gain penalty imposed on RSOA compared to SOA providing the same small-signal gain. This gain reduction for RSOA, in the order of 1~2 dB, will happen in almost all practical conditions, including the situation when the input signals are weak and fast. This phenomenon is the consequence of a higher optical intensity in RSOA, due to its rear-facet reflection. Moreover, the effect of carrier re-pumping, observed as additional distortions on the trailing edge of output pulses, occurs more easily with RSOA. The interplay of these two mechanisms results in a time delay which could be substantially different for RSOA and SOA operating in similar conditions. The output waveforms from these two devices easily diverge as well, even though their respective spectra remain similar in most situations.

The device model and the associated algorithm used in this study are readily applicable to pulse trains. It is demonstrated that both SOA and RSOA can still provide substantial power gains to fast PCM signals (up to 40 Gb/s) in spite of the patterning effect.

The above knowledge might be potentially important if RSOAs are to be deployed in communication networks or in other applications, in which signal synchronization is a key issue.

The nonlinear interactions studied in this paper usually require adequate simulation tools. The numerical method adopted here, together with its associated algorithm, might be a promising candidate for SOA and RSOA modeling, due to its demonstrated precision and its flexibility for input signals.

VI. Acknowledgement

The author acknowledges insightful discussions with his colleagues, Dr. Pascal Morel and Pr. Ammar Sharaiha. He also thanks Pr. Chao Lu from Polytechnic University of Hong Kong for technical supports.

References

[1] G. de Valicourt, D. Maké J. Landreau, M. Lamponi, G. H. Duan, P. Chanclou, and R. Brenot, "High gain (30dB) and high saturation power (11 dBm) RSOA devices as colorless ONU sources in long-reach hybrid WDM/TDM-PON architecture," *IEEE Photonics Technology Letters*, vol. 22, pp. 191-193, Feb. 1, 2010.

[2] L. Yi, Z. Li, Y. Dong, S. Xiao, J. Chen, and W. Hu, "Upstream capacity upgrade in TDM-PON using RSOA based tunable fiber ring laser", *Optics Express*, vol. 20, no. 9, pp. 10416-10425, 2012.

[3] M. J. Connelly, "Reflective semiconductor optical amplifier pulse propagation model," *IEEE Photonics Technology Letters*, vol. 24, no. 2, pp. 95-97, Jan. 15, 2012.

[4] G. P. Agrawal and N. A. Olsson, "Self-phase modulation and spectral broadening of optical pulses in semiconductor laser amplifiers," *IEEE J. Quantum Electron.*, vol. 25, pp. 2297-2306, Nov. 1989.

[5] J. W. D. Chi, A. Fernandez, and C. Lu, "A comprehensive modeling of wave propagation in photonic devices," *IET Commun*., vol. 6, no. 5, pp. 571-576, 2012.

[6] J. W. D. Chi, A. Fernandez, and C. Lu, "Properties of mode-locked optical pulses in a dispersion-managed fiber-ring laser using semiconductor optical amplifier as active device," *IEEE J. Quantum Electron.*, vol. 49, no. 1, pp. 80-88, Jan. 2013.

[7] A. V. Uskov, T. W. Berg, and J. Mørk, "Theory of pulse-train amplification without patterning effects in quantum-dot semiconductor optical amplifiers," *IEEE J. Quantum Electron.*, vol. 40, no. 3, pp. 306-320, Mar. 2004.

[8] P. Morel and A. Sharaiha, "Wideband time-domain transfer matrix model equivalent circuit for short pulse propagation in semiconductor optical amplifiers," *IEEE J. Quantum Electron.*, vol. 45, no. 2, pp. 103-116, Feb. 2009.